

1 **Title page**

2 **i. Title**

3 Monitoring the seasonal functioning of tropical ecosystems with phenocams

4 **ii. Full name of the authors**

5 Adeline Fayolle<sup>1,2,3\*</sup>, Léna Royen<sup>1</sup>, Emma Bush<sup>4</sup>, Nassim Daher<sup>1</sup>, Sébastien Dandrifosse<sup>1</sup>, Anais  
6 Gorel<sup>1,5</sup>, David Lehmann<sup>6,7,8</sup>, Loïc Makaga<sup>6</sup>, Benoît Mercatoris<sup>1</sup>, Katharine Abernethy<sup>3,8</sup>

7 Corresponding author: Adeline Fayolle

8 **iii. Affiliations**

9 <sup>1</sup> Gembloux Agro-Bio Tech, University of Liège, Belgium

10 <sup>2</sup> Cirad, Montpellier, France

11 <sup>3</sup> Institut de Recherche en Ecologie Tropicale, CENAREST, Gabon

12 <sup>4</sup> Royal Botanic Garden Edinburgh, UK

13 <sup>5</sup> Faculty of Bioscience Engineering, Ghent University, Belgium

14 <sup>6</sup> Agence National des Parcs Nationaux, Gabon

15 <sup>7</sup> Okala, Gabon

16 <sup>8</sup> University of Stirling, UK

17 \* corresponding author : [adeline.fayolle@cirad.fr](mailto:adeline.fayolle@cirad.fr)

18 **iv. Abstract and keywords**

19 Abstract: Phenology is an essential biodiversity variable, but land surface phenology is challenging in  
20 cloudy tropical regions while field observations are time-consuming and sparse in time. Phenocams  
21 offer opportunities that have been barely explored in Africa. Here, we present the first results of a  
22 phenocam network installed in Gabon. The two years of images show the seasonal and bimodal  
23 functioning of forest canopy, mimicking rainfall seasonality, and the unimodal functioning of savanna,  
24 associated with the long dry season and fire. This work is encouraging though the challenge is to  
25 maintain phenocams over the long-term and automate the signal analysis.

26

27 Keywords: Deciduousness, Dry season, Greenness, Phenology

28

29 Conflict of Interest Statement: The authors do not have any conflict of interest to declare.

30

## 31 v. Main text

### 32 1. Introduction

33 A myriad of growth and life strategies have been identified in the tropics (Abernethy, Bush, Forget,  
34 Mendoza, & Morellato, 2018; Sakai, 2001) encompassing irregular and regular phenologies, and among  
35 them, sub-annual, annual, supra-annual and continuous patterns (Newstrom, Frankie, & Baker, 1994).  
36 Annual cycles were found to dominate in a cross-site analysis of flowering across tropical Africa  
37 (Adamescu et al., 2018) and in specific sites, Lopé National Park (NP) in Gabon (Bush et al., 2017) and  
38 Luki Biosphere Reserve (BR) in the Democratic Republic of the Congo (Angoboy Ilondea et al., 2019).  
39 Central African tropical forest canopies also show a high proportion of fully deciduous trees and a strong  
40 seasonal functioning (Gond et al., 2013; Philippon et al., 2019). The important deciduousness of tropical  
41 forests in central Africa is probably due to their drier climates in comparison with the other tropical  
42 regions (Guan et al., 2015).

43 Vegetative phenology has been historically less studied than reproductive phenology in central  
44 Africa because earlier studies were related to animal diet and focused on fruiting (Brugiere, Gautier,  
45 Mougazi, & Gautier-Hion, 2002; Tutin, Williamson, Rogers, & Fernandez, 1991; White, 1994). Also,  
46 since field observations are extremely time-consuming, phenology surveys target a few individuals  
47 monitored at a low temporal resolution (usually once a month) not suitable to capture quick changes in  
48 leaf phenology (Bush et al., 2018). Leaf renewal can be extremely rapid with one week between leaf  
49 shedding and unfolding for *Prioria balsamifera* in Luki BR (Angoboy Ilondea et al., 2021), a relatively dry  
50 site (c. 1,200 mm yr<sup>-1</sup> rainfall) at the southern tip of the moist forest biome (Aleman et al., 2020). In  
51 addition, the dense cloud cover that allows persistence of forests under dry and seasonal climates in  
52 central Africa (Philippon et al., 2019) also prevents analyses using satellite observations (Adole, Dash,  
53 & Atkinson, 2018). Other approaches are thus required to monitor canopy seasonality which is of great  
54 importance to unravel ecosystem functioning and responses to seasonal drought. Near-surface remote  
55 sensing, *i.e.*, images automatically collected at high temporal frequency from fixed-point by digital  
56 cameras, started almost two decades ago (Richardson et al., 2007) and allowed to investigate the  
57 seasonality of trees and forest ecosystems worldwide (Brown et al., 2016). In the tropics, the coverage  
58 is still limited, but there is a huge potential for the expansion of networks that already encompass a  
59 variety of vegetation types such as the cerrado (Alberton et al., 2014) and other seasonally dry tropical  
60 communities (Alberton et al., 2019) of Brazil, and tropical forests as done in the central Amazon (Lopes  
61 et al., 2016) and in Borneo (Nagai et al., 2016). The phenological monitoring of African trees is probably  
62 different from trees in other forested ecosystems, both tropical and temperate, because of the high  
63 seasonal functioning (Gond et al., 2013), and the coexistence of evergreen and semi-deciduous species  
64 in the canopy (Gorel et al., 2025). Yet, only few studies in central Africa investigated leaf phenology, but  
65 see Angoboy Ilondea et al., (2021) in Luki, and Kearsley et al., (2024) in Yangambi.

66 In this study, our aim is to show the potential of using phenocams to monitor the seasonal  
67 functioning of tropical trees and ecosystems in central Africa. We present a methodological approach  
68 developed for the processing of phenocam images taken in the forest-savanna mosaic landscape found  
69 at the northern and eastern limits of Lopé NP and where the ecotone forms a distinct tree community

70 (Cardoso et al., 2021). The site is located near the Equator (Figure 1) and shows a bimodal distribution  
71 of monthly rainfall (Bush, Jeffery, et al., 2020). We tested this approach by addressing the following  
72 research questions. 1) To what extent canopy greenness shows a seasonal trend that is related to  
73 climate seasonality? 2) Do forests and savannas show similar trends in greenness seasonality? Indeed,  
74 distinct leaf phenology strategies have been demonstrated for forest and savannas and interpreted as  
75 a temporal niche separation (Higgins, Delgado-Cartay, February, & Combrink, 2011).

## 76 **2. Material and methods**

### 77 *2.1 Phenocam images*

78 A total of 12 Moultrie Wingscapes TimelapseCam Pro were installed on trees between September 2019  
79 and November 2021 near the “Station d’Etudes des Gorilles et des Chimpanzés” (SEGC, Figure 1). For  
80 the camera deployment in the field, we used the topography to maximise the view on forest patches  
81 given the device used and which has lens field of view of 40°. The phenocams were mounted on trees  
82 or poles at 1-2 m height, and were parametrized to collect two JPEG images (6080 × 3420 pixels, ~ 3  
83 Mo) each day at 11 and 12 am to limit the influence of the sun angle (Alberton et al., 2017). We recognize  
84 that more images would have been better, but we first let the phenocams running during one year without  
85 any maintenance. Eight AA lithium batteries per camera powered image acquisition for one year. After  
86 the first year when cameras were rarely checked and suffered changes in the field of view, we changed  
87 the protocol to check phenocams every three months. In this study, we focused on the three phenocams  
88 with the longest time series, phenocams 005, 006 and 007, which collected 1,465, 1,181 and 1,459  
89 images, respectively, from the 24<sup>th</sup> of September 2019 to the 22<sup>th</sup> of September 2021. The number of  
90 images differs due to technical problems related to wind or maintenance.

### 91 *2.2 Rainfall and temperature*

92 Weather data were acquired onsite during the period covered by the phenocam images at the SEGC  
93 (11.605 E, -0.201 N) and the weather station is located in a savanna environment (Bush, Jeffery, et al.,  
94 2020). A manual rain gauge recorded total daily rainfall at 8 am each morning. Daily temperature was  
95 recorded automatically using a TinyTag Plus 2 data logger (Gemini Data Loggers  
96 <https://www.geminidataloggers.com/data-loggers/tinytag-plus-2>, some of which record both  
97 temperature and relative humidity). The timeseries is however incomplete for temperature with five  
98 missing months in 2021. Onsite daily rainfall data showed annual rainfall of 1,555 mm, 1,365 mm, and  
99 1,765 mm, respectively for 2019, 2020, 2021, in line with the trends observed between 1984 and 2018,  
100 with a mean annual rainfall of 1,500 mm (Bush, Jeffery, et al., 2020) and biannual cycles with two rainy  
101 (March-April-May and October-November) and dry (June-July-August-September and December-  
102 January-February) seasons (Figure 1b). The short dry season is known to be less dry and more variable  
103 than the long dry season which is very consistent (Bush, Jeffery, et al., 2020) and light-deficient  
104 (Philippon et al., 2019).

### 105 2.3 Images processing

106 We developed a framework for processing the phenocam images and the first step consists of selecting  
107 a reference image that fixes the field of view (step 1, Figure 2). Regions Of Interest (ROIs), such as the  
108 extent of the forest and savanna, are then manually drawn in QGIS by visual interpretation of the  
109 reference image. Since the angle of view fluctuated, the reference image was used to align all other  
110 images (step 2). This was carried out via a python code developed previously (Dandrifosse, Carlier,  
111 Dumont, & Mercatoris, 2021) and combining the A-KAZE and ECC methods implemented in the  
112 OpenCV-Python library (version 4.1.0.25 and Python 3.7). The feature-based A-KAZE algorithm was  
113 first used to roughly align images with the reference image, as required for the ECC method. A-KAZE is  
114 based on key points selected for their invariance to change in brightness, contrast, scale, or rotation,  
115 which are employed as corresponding points during the alignment process between the input image and  
116 the reference image. Then, the ECC algorithm estimates the geometric transformation (warp) between  
117 the input and the reference image and returns a warped input image close to the reference image. After  
118 alignment, poor-quality images due to heavy rainfall, dense clouds, and/or faulty alignments were  
119 removed manually (step 3) and areas not common to the reference image (black edge stripes) were  
120 removed in R (step 4), which was also used for subsequent steps.

121 We then calculated the Green Chromatic Coordinate (GCC) for each pixel in each image (step 5).

$$122 \text{GCC} = G / (R + G + B) \quad (1)$$

123 where G, R and B are the red, green and blue digital numbers corresponding to the intensity of each  
124 primary colour. The GCC is the most widely used 'chromatic coordinates' index for extracting  
125 phenological information from RGB channels (Gillespie et al., 1987), being effective for extracting leaf  
126 colour changes and getting rid of light variation (Sonnentag et al., 2012) including in tropical regions  
127 (Alberton et al., 2014, 2019; Lopes et al., 2016). Afterwards, the GCC values were averaged for each  
128 ROI in each image (step 6).

### 129 2.4 Data analyses

130 To reduce the noise in the GCC data and to detect seasonal trends in GCC time series, we explored  
131 several smoothing approaches such as moving average. Here, we show the results of fitted Generalized  
132 Additive Mixed Models (GAMMs) that were used previously in phenology analyses based on field  
133 observations (Polansky & Robbins, 2013) and on GCC timeseries from phenocam images (Alberton et  
134 al., 2019). This was done separately for the forest and savanna ROIs using the restricted maximum  
135 likelihood smoothing method and setting the number of basic functions to 15. The GCC timeseries were  
136 related to climate seasonality, and specifically to monthly rainfall and average temperature. The two  
137 variables were combined for the whole period in the style of a Walter-Lieth climate diagram. In such  
138 diagram a dry month corresponds to monthly rainfall below twice the average temperature (approx. 50  
139 mm and 25°C, respectively) and a very wet month corresponds to more than 100 mm rainfall. All  
140 analyses were done in R using the following packages: *raster* for image processing (Hijmans, 2017),  
141 *lubridate* for dealing with dates (Spinu et al., 2024), *dplyr* for data management (Wickham et al., 2023),  
142 *mgcv* for fitting GAMM models (Wood, 2025), and *climatol* for the climatic diagram (Gujjarro, 2025).

143 **3. Results**

144 We first explored the seasonality of canopy greenness and local climate. Variation in GCC for the forest  
145 ROI was bimodal for phenocams 006 and 007 (Figure 3b and c) and the peaks occurred during the rainy  
146 seasons (in blue) and troughs during the dry seasons (in red, on the climatic diagram reported for the  
147 whole study period, Figure 3d). The larger trough occurred at the end of the long dry season which lasts  
148 from June to September. This bimodal trend in forest greenness was less clear for the phenocam 005  
149 probably because the peak in greenness was earlier than the start of monitoring (Figure 3a). Also, the  
150 data recorded by this phenocam were noisier with large daily and weekly variations (Figure 3a), perhaps  
151 because of camera calibration. The GCC varied between 0.28 and 0.41 for this specific phenocam, while  
152 the GCC variation was much more restricted, between 0.32 and 0.36, for phenocams 006 and 007.

153 We then explored whether the savannas show the same trend in greenness seasonality as the  
154 forest patches. For the savanna ROIs, the GCC shows a broad peak from October to November which  
155 corresponds to the rainy season, and this peak can last until December, January and February, the  
156 short dry season (Figure 3b, c and d), during which the GCC starts decreasing to a minimum value  
157 observed at the end of the long dry season, when savanna fires are initiated onsite. Savanna fires were  
158 recorded for the phenocams 006 (no fire in 2020, burnt on the 27<sup>th</sup> of August 2021, Figure 3b) and 007  
159 (burnt on the 8<sup>th</sup> of September 2020 and on the 28<sup>th</sup> of August 2021, Figure 3c). Shortly after burning,  
160 savanna GCC values sharply increased and followed the same cycle. For the same phenocam, the  
161 range of GCC values was larger for the savanna than for the forest ROI (Figure 3).

162 **4. Discussion**

163 The two years of images taken by three phenocams in Lopé NP provided encouraging results confirming  
164 the potential of this technology to monitor the seasonal functioning of tropical ecosystems in central  
165 Africa. In addition, these results highlight the diversity of patterns found in the forest-savanna mosaic  
166 landscape since our phenocams recorded both the biannual forest green-up cycle, aligned with monthly  
167 rainfall distribution, and the annual savanna green-up cycle, aligned with the long dry season and the  
168 savanna burning (Jeffery et al., 2014). The amount of data from the three timeseries analyzed so far  
169 and including a complete year and a second one with missing data, is comparable to the few published  
170 studies in tropical forests, based on a single phenocam mounted on a tower and running over one year  
171 in the central Amazon (Lopes et al., 2016) and over two years in Borneo (Nagai et al., 2016).

172 In contrast to satellite observations that are made over wide areas, but at low spatial and  
173 temporal resolutions, near-surface remote sensing offers observations at the scale of tree crowns and  
174 at a high temporal resolution as earlier developed globally (Brown et al., 2016) and for the tropics  
175 (Alberton et al., 2017). Here, we demonstrated that it is possible to use devices that are cheap and easy  
176 to set up, and with a minimum parametrisation of only two images a day, we found a bimodal signal in  
177 forest greenness, a trend that was previously detected with the Enhanced Vegetation Index of MODIS  
178 satellite further inland (Gond et al., 2013) and across the region (Philippon et al., 2019). With two  
179 greenness peaks during the rainy seasons, canopy functioning appeared relatively seasonal for an  
180 evergreen forest belonging to the “Atlantic inland evergreen domain” of Réjou-Méchain et al. (2021),

181 probably because the canopy still holds deciduous species (Bush, Mitchard, et al., 2020). Greenness is  
182 minimum during the long dry season and only a slowdown is observed during the short rainy season,  
183 when both fruit quantity and diversity peak onsite (White, 1994). In Lambir NP in Malaysia where rainfall  
184 is greater (2,600 mm yr<sup>-1</sup>), no seasonal trend was detected at the whole canopy level (Nagai et al., 2016)  
185 but leaf colouring and flowering were observed at the crown level. In the central Amazon, highly seasonal  
186 with a sunny dry season, rapid large-amplitude negative/positive changes in GCC for individual tree  
187 crowns were interpreted as leaf loss/flush events (Lopes et al., 2016). The diversity of leaf phenology  
188 strategies remains to be explored, and requires a tree crown approach.

189 Here, we developed a framework for the processing of phenocam images. The alignment  
190 approach we employed, combining the A-KAZE and ECC algorithms, introduces a novel and  
191 straightforward method for generating timeseries within regions of interest (ROIs). This method earlier  
192 developed by Dandrifosse et al., (2021) effectively addresses perspective shifts, which can frequently  
193 occur due to maintenance routines, data downloads, or environmental conditions. However, although  
194 these algorithms effectively handle minor deviations in viewing angles, substantial shifts in the camera's  
195 perspective can, on occasion, lead to significant pixel loss. Consequently, we strongly recommend  
196 securely fastening camera mounts to guarantee a consistently stable field of vision over time. For the  
197 deployment of new phenocams, it is essential to use a stable support (metal stake, telephone pole) and  
198 fixation ties that are resistant to temperature and humidity variations. Similarly, ensuring that growing  
199 vegetation does not obstruct the field of view is vital. Regular maintenance (every three months onsite)  
200 should include clearing vegetation from the phenocam's field of view and minimizing phenocam  
201 manipulation to prevent movements and misalignment with the reference scene. It is also important to  
202 protect the phenocam against lightning which is frequent in the tropics and in central Africa (Albrecht,  
203 Goodman, Buechler, Blakeslee, & Christian, 2016). Two of our phenocams were indeed destroyed by  
204 lightning in December 2021. We developed our approach with open-source tools (QGIS, python, and R)  
205 but for user convenience, we intend to develop the analysis pipeline into a single program (and  
206 language), likely python or R, the latter already includes several packages dedicated to the analyses of  
207 phenocam images. We also intend to develop an interface to aid phenophase photointerpretation for  
208 individual tree crowns, with the potential to undertake species level observation for dominant canopy  
209 species. This would facilitate calibration datasets for algorithm development. In comparison with other  
210 devices, the cameras we used are relatively cheap (125€), easy to parametrize and to set up, and can  
211 be implemented for phenology monitoring in extremely remote areas, since camera and image file  
212 format have been shown to be of secondary influence (Sonnentag et al., 2012). To better filter the signal,  
213 it would be desirable to increase the number of pictures per day. Taking into account the data storage  
214 capacity of Wingscapes TimelapseCam Pro, a shooting time spanning 10 to 14 hours (Alberton et al.,  
215 2014), along with quarterly battery replacement and data archiving practices, we estimate that the image  
216 capture rate could reach as high as one image every three minutes with a maximum SD card of 32 Go  
217 (imposed by the phenocam model) and an average image size of 3.3 Mo (4 hours of image capture, 20  
218 images per hour over 90 days leads to 23.2 Go). Finally, the data gaps in the time series analysed are  
219 unfortunate, but increasing the frequency of maintenance is difficult. Solutions for real-time data transfer  
220 needs to be explored, but are not yet feasible in many places of central Africa.

221 To conclude, the approach outlined in this study, along with the cost-effectiveness and suitability  
222 of phenocams for remote deployment, establishes them as a highly promising tool for researchers  
223 committed to investigating environmental changes in tropical forests and savannas across Africa and  
224 the global tropics, where advance and apply phenological research is urgently needed (Sullivan et al.,  
225 2023).

226

## 227 **vi. Acknowledgments**

228 The authors thank the FNRS-FRIA for funding the PhD fellowship of Nassim Daher during which the  
229 phenocams were installed. AF and KA also thank the FNRS for funding the CANOPi project, under the  
230 EOS Call (grant number O.0026.22). The SEGC research station (KA, DL, LM) received core funding  
231 from Total Gabon for staff maintenance of the phenocams and datasets during 2019-2020. Anaïs Gorel  
232 was supported by the Special Research Fund Ghent University—BOF postdoctoral fellowship  
233 BOF20/PDO/003.

## 234 **vii. Data Availability Statement**

235 The raw data (images and time series) and R codes will be made available upon request.

## 236 **viii. References**

- 237 Abernethy, K., Bush, E. R., Forget, P.-M., Mendoza, I., & Morellato, L. P. C. (2018). Current issues in  
238 tropical phenology : A synthesis. *Biotropica*, *50*(3), 477-482.
- 239 Adamescu, G. S., Plumptre, A. J., Abernethy, K. A., Polansky, L., Bush, E. R., Chapman, C. A., ...  
240 Beale, C. M. (2018). Annual cycles are the most common reproductive strategy in African  
241 tropical tree communities. *Biotropica*, *50*(3), 418-430. doi: 10.1111/btp.12561
- 242 Adole, T., Dash, J., & Atkinson, P. M. (2018). Characterising the land surface phenology of Africa using  
243 500 m MODIS EVI. *Applied Geography*, *90*, 187-199.
- 244 Alberton, B., Almeida, J., Helm, R., Torres, R. da S., Menzel, A., & Morellato, L. P. C. (2014). Using  
245 phenological cameras to track the green up in a cerrado savanna and its on-the-ground  
246 validation. *Ecological Informatics*, *19*, 62-70.
- 247 Alberton, B., da Silva Torres, R., Sanna Freire Silva, T., Rocha, H. R. da, SB Moura, M., & Morellato, L.  
248 P. C. (2019). Leafing patterns and drivers across seasonally dry tropical communities. *Remote*  
249 *Sensing*, *11*(19), 2267.
- 250 Alberton, B., Torres, R. da S., Cancian, L. F., Borges, B. D., Almeida, J., Mariano, G. C., ... Morellato,  
251 L. P. C. (2017). Introducing digital cameras to monitor plant phenology in the tropics :  
252 Applications for conservation. *Perspectives in Ecology and Conservation*, *15*(2), 82-90.
- 253 Albrecht, R. I., Goodman, S. J., Buechler, D. E., Blakeslee, R. J., & Christian, H. J. (2016). Where Are  
254 the Lightning Hotspots on Earth? *Bulletin of the American Meteorological Society*, *97*(11),  
255 2051-2068. doi: 10.1175/BAMS-D-14-00193.1

256 Aleman, J. C., Fayolle, A., Favier, C., Staver, A. C., Dexter, K. G., Ryan, C. M., ... Chidumayo, E. N.  
257 (2020). Floristic evidence for alternative biome states in tropical Africa. *Proceedings of the*  
258 *National Academy of Sciences*, 117(45), 28183-28190.

259 Angoboy Ilondea, B., Beeckman, H., Ouedraogo, D.-Y. O., Bourland, N., De Mil, T., Van Den Bulcke,  
260 J., ... Hubau, W. (2019). Une forte saisonnalité du climat et de la phénologie reproductive dans  
261 la forêt du Mayombe : L'apport des données historiques de la Réserve de Luki en République  
262 démocratique du Congo. *Bois et Forêts des Tropiques*, 341, 39-53.

263 Angoboy Ilondea, B., Beeckman, H., Van Acker, J., Van den Bulcke, J., Fayolle, A., Couralet, C., ...  
264 Kaka di-Makwala, A. (2021). Variation in onset of leaf unfolding and wood formation in a Central  
265 African tropical tree species. *Frontiers in Forests and Global Change*, 4.

266 Brown, T. B., Hultine, K. R., Steltzer, H., Denny, E. G., Denslow, M. W., Granados, J., ... SanClements,  
267 M. (2016). Using phenocams to monitor our changing Earth : Toward a global phenocam  
268 network. *Frontiers in Ecology and the Environment*, 14(2), 84-93.

269 Brugiére, D., Gautier, J.-P., Mougazi, A., & Gautier-Hion, A. (2002). Primate diet and biomass in  
270 relation to vegetation composition and fruiting phenology in a rain forest in Gabon. *International*  
271 *Journal of Primatology*, 23(5), 999-1024.

272 Bush, E. R., Abernethy, K. A., Jeffery, K., Tutin, C., White, L., Dimoto, E., ... Bunnefeld, N. (2017).  
273 Fourier analysis to detect phenological cycles using long-term tropical field data and  
274 simulations. *Methods in Ecology and Evolution*, 8(5), 530-540.

275 Bush, E. R., Bunnefeld, N., Dimoto, E., Dikangadissi, J.-T., Jeffery, K., Tutin, C., ... Abernethy, K. A.  
276 (2018). Towards effective monitoring of tropical phenology : Maximizing returns and reducing  
277 uncertainty in long-term studies. *Biotropica*, 50(3), 455-464.

278 Bush, E. R., Jeffery, K., Bunnefeld, N., Tutin, C., Musgrave, R., Moussavou, G., ... Ndong, J. E. (2020).  
279 Rare ground data confirm significant warming and drying in western equatorial Africa. *PeerJ*, 8,  
280 e8732.

281 Bush, E. R., Mitchard, E. T., Silva, T. S., Dimoto, E., Dimbonda, P., Makaga, L., & Abernethy, K. (2020).  
282 Monitoring mega-crown leaf turnover from space. *Remote Sensing*, 12(3), 429.

283 Cardoso, A. W., Oliveras, I., Abernethy, K. A., Jeffery, K. J., Glover, S., Lehmann, D., ... Malhi, Y. (2021).  
284 A distinct ecotonal tree community exists at central African forest–savanna transitions. *Journal*  
285 *of Ecology*, 109(3), 1170-1183. doi: 10.1111/1365-2745.13549

286 Dandrifosse, S., Carlier, A., Dumont, B., & Mercatoris, B. (2021). Registration and Fusion of Close-  
287 Range Multimodal Wheat Images in Field Conditions. *Remote Sensing*, 13(7), 1380.

288 Gillespie, A. R., Kahle, A. B., & Walker, R. E. (1987). Color enhancement of highly correlated images.  
289 II. Channel ratio and "chromaticity" transformation techniques. *Remote Sensing of Environment*,  
290 22(3), 343-365.

291 Gond, V., Fayolle, A., Pennec, A., Cornu, G., Mayaux, P., Camberlin, P., ... Gourlet-Fleury, S. (2013).  
292 Vegetation structure and greenness in Central Africa from Modis multi-temporal data.  
293 *Philosophical Transactions of the Royal Society B: Biological Sciences*, 368(1625), 20120309.

294 Gorel, A., Fayolle, A., Ligot, G., Rossi, V., Hardy, O. J., Beeckman, H., & Steppe, K. (2025). Leaf habit,  
295 maximum height and wood density of tropical woody flora in Africa : Phylogenetic constraints,

296 covariation and responses to seasonal drought. *Journal of Ecology*, 113(5), 1209-1224. doi:  
297 10.1111/1365-2745.70027

298 Guan, K., Pan, M., Li, H., Wolf, A., Wu, J., Medvigy, D., ... Malhi, Y. (2015). Photosynthetic seasonality  
299 of global tropical forests constrained by hydroclimate. *Nature Geoscience*, 8(4), 284-289.

300 Guijarro, J. A. (2025). *climatol: Climate Tools (Series Homogenization and Derived Products)*. Consulté  
301 à l'adresse <https://lib.stat.cmu.edu/R/CRAN/web/packages/climatol/>

302 Higgins, S. I., Delgado-Cartay, M. D., February, E. C., & Combrink, H. J. (2011). Is there a temporal  
303 niche separation in the leaf phenology of savanna trees and grasses? *Journal of Biogeography*,  
304 38(11), 2165-2175.

305 Hijmans, R. J. (2017). *raster: Geographic Data Analysis and Modeling*. Consulté à l'adresse  
306 <https://CRAN.R-project.org/package=raster>

307 Jeffery, K. J., Korte, L., Palla, F., Walters, G. M., White, L., & Abernethy, K. (2014). Fire management  
308 in a changing landscape: A case study from Lopé National Park, Gabon. *PARKS. The*  
309 *International Journal of Protected Areas and Conservation*, 20(1), 39-52.

310 Kearsley, E., Verbeeck, H., Stoffelen, P., Janssens, S. B., Yakusu, E. K., Kosmala, M., ... Hufkens, K.  
311 (2024). Historical tree phenology data reveal the seasonal rhythms of the Congo Basin  
312 rainforest. *Plant-Environment Interactions*, 5(2), e10136. doi: 10.1002/pei3.10136

313 Lopes, A. P., Nelson, B. W., Wu, J., de Alencastro Graça, P. M. L., Tavares, J. V., Prohaska, N., ...  
314 Saleska, S. R. (2016). Leaf flush drives dry season green-up of the Central Amazon. *Remote*  
315 *Sensing of Environment*, 182, 90-98.

316 Nagai, S., Ichie, T., Yoneyama, A., Kobayashi, H., Inoue, T., Ishii, R., ... Itioka, T. (2016). Usability of  
317 time-lapse digital camera images to detect characteristics of tree phenology in a tropical  
318 rainforest. *Ecological Informatics*, 32, 91-106.

319 Newstrom, L. E., Frankie, G. W., & Baker, H. G. (1994). A new classification for plant phenology based  
320 on flowering patterns in lowland tropical rain forest trees at La Selva, Costa Rica. *Biotropica*,  
321 141-159.

322 Philippon, N., Cornu, G., Monteil, L., Gond, V., Moron, V., Pergaud, J., ... Ngomanda, A. (2019). The  
323 light-deficient climates of western Central African evergreen forests. *Environmental Research*  
324 *Letters*, 14(3), 034007. doi: 10.1088/1748-9326/aaf5d8

325 Polansky, L., & Robbins, M. M. (2013). Generalized additive mixed models for disentangling long-term  
326 trends, local anomalies, and seasonality in fruit tree phenology. *Ecology and Evolution*, 3(9),  
327 3141-3151.

328 Réjou-Méchain, M., Mortier, F., Bastin, J.-F., Cornu, G., Barbier, N., Bayol, N., ... Gourlet-Fleury, S.  
329 (2021). Unveiling African rainforest composition and vulnerability to global change. *Nature*,  
330 593(7857), 90-94. doi: 10.1038/s41586-021-03483-6

331 Richardson, A. D., Jenkins, J. P., Braswell, B. H., Hollinger, D. Y., Ollinger, S. V., & Smith, M.-L. (2007).  
332 Use of digital webcam images to track spring green-up in a deciduous broadleaf forest.  
333 *Oecologia*, 152(2), 323-334. doi: 10.1007/s00442-006-0657-z

334 Sakai, S. (2001). Phenological diversity in tropical forests. *Population ecology*, 43(1), 77-86.

335 Sonnentag, O., Hufkens, K., Teshera-Sterne, C., Young, A. M., Friedl, M., Braswell, B. H., ...  
336 Richardson, A. D. (2012). Digital repeat photography for phenological research in forest  
337 ecosystems. *Agricultural and Forest Meteorology*, 152, 159-177.

338 Spinu, V., Grolemond, G., Wickham, H., Vaughan, D., Lyttle, I., Costigan, I., ... Lee, C. H. (2024).  
339 *lubridate: Make Dealing with Dates a Little Easier*. Consulté à l'adresse  
340 <https://lib.stat.cmu.edu/R/CRAN/web/packages/lubridate/>

341 Sullivan, M. K., Fayolle, A., Bush, E., Ofori-Bamfo, B., Vleminckx, J., Metz, M. R., & Queenborough, S.  
342 A. (2023). Cascading effects of climate change : New advances in drivers and shifts of tropical  
343 reproductive phenology. *Plant Ecology*. doi: 10.1007/s11258-023-01377-3

344 Tutin, C., Williamson, E., Rogers, M., & Fernandez, M. (1991). A case study of a plant-animal  
345 relationship : *Cola lizae* and lowland gorillas in the Lope Reserve, Gabon. *Journal of Tropical*  
346 *Ecology*, 181-199.

347 White, L. J. (1994). Patterns of fruit-fall phenology in the Lopé Reserve, Gabon. *Journal of Tropical*  
348 *Ecology*, 289-312.

349 Wickham, H., François, R., Henry, L., Müller, K., Vaughan, D., Software, P., & PBC. (2023). *dplyr: A*  
350 *Grammar of Data Manipulation*. Consulté à l'adresse  
351 <https://lib.stat.cmu.edu/R/CRAN/web/packages/dplyr/>

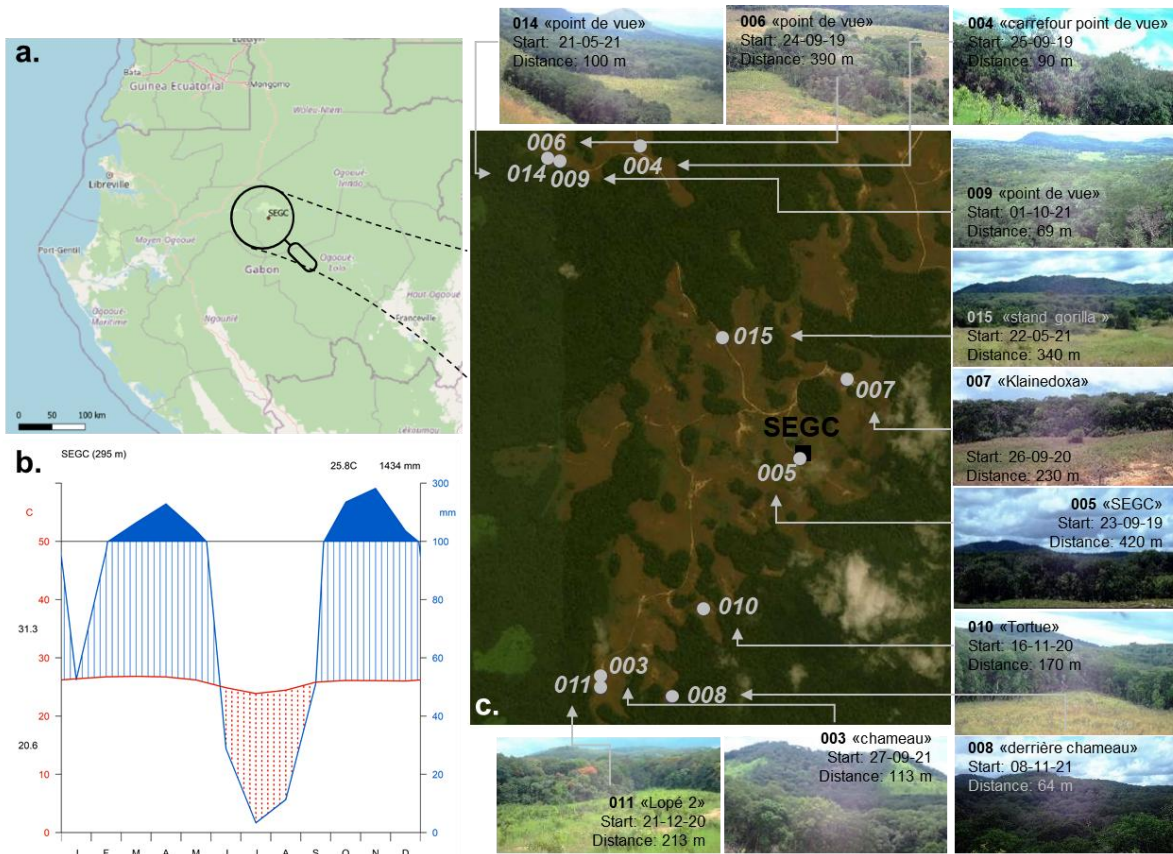
352 Wood, S. (2025). *mgcv: Mixed GAM Computation Vehicle with Automatic Smoothness Estimation*.  
353 Consulté à l'adresse <https://lib.stat.cmu.edu/R/CRAN/web/packages/mgcv/>

354  
355

356 ix. Tables (each table complete with title and footnotes)

357 x. Figures

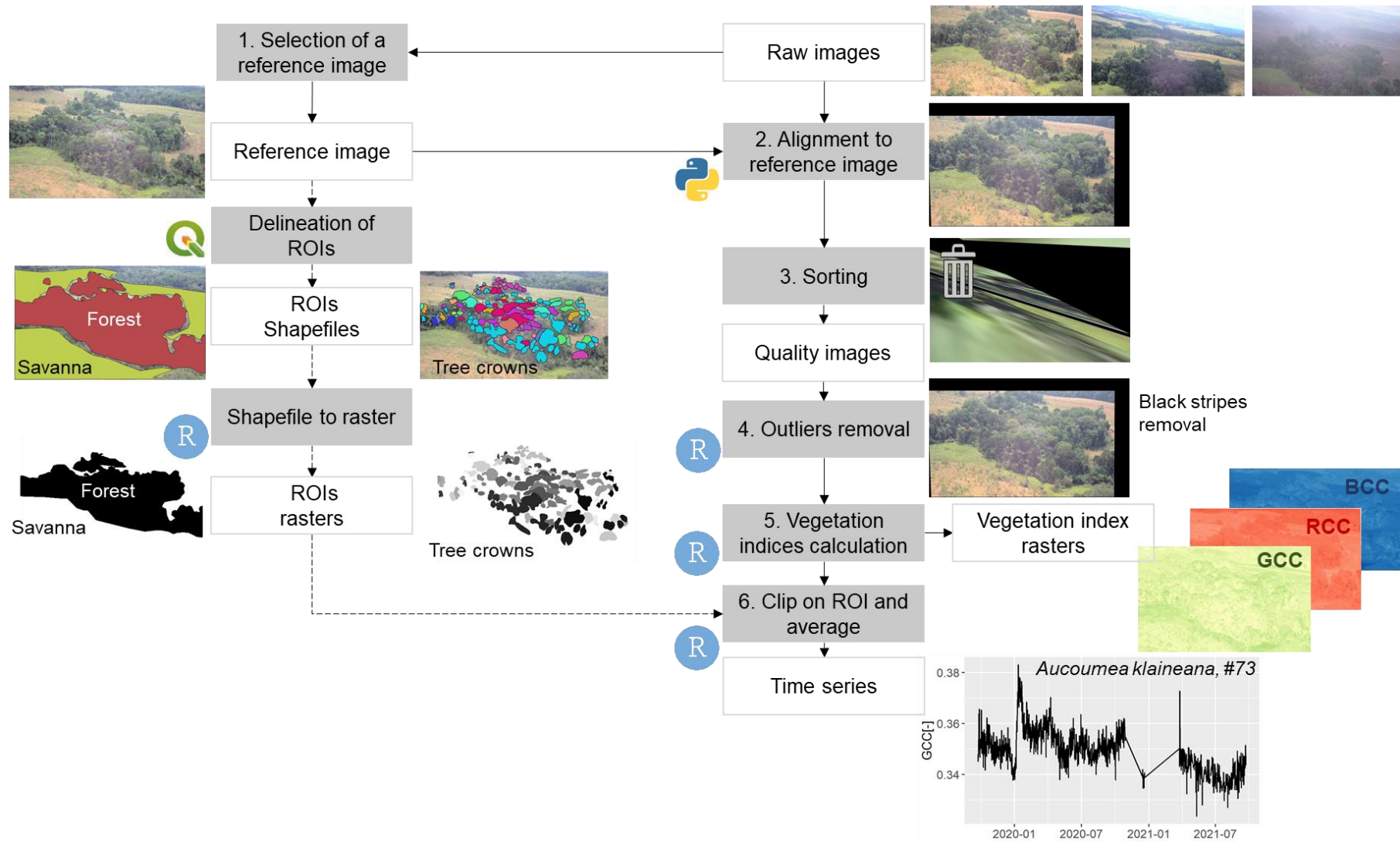
358 Figure 1. Phenocams installed in Lopé NP, Gabon. The location of the “Station d’Etudes des Gorilles et  
359 des Chimpanzés” (SEGC) is shown in Gabon (a) and the Walter–Lieth diagram showing rainfall (in blue)  
360 and temperature (in red) is provided (b). The phenocams installed in the field are also located with their  
361 respective reference image (c).



362

363

364 Figure 2. Analytical framework developed for the processing of phenocam images. The software used, either QGIS, Python or R is indicated with the respective  
 365 logo.



366 Figure 3. Variation of the Green Chromatic Coordinates (GCC, dimensionless) for the three phenocams,  
 367 005 (a), 006 (b) and 007 (c), installed at Lopé NP and for which a two-year time series is available. The  
 368 reference images are shown as inset. The lines correspond to the predictions of a GAMM model fitted  
 369 separately for the forest (green) and savanna (yellow) on the ROI average for each image (one cross).  
 370 (d) Monthly cumulative rainfall amounts (in red) and daily average temperature (in blue) throughout time  
 371 are presented in the style of a Walter-Lieth climate diagram. Dry seasons occur when the rainfall curve  
 372 falls below the temperature curve (shown as the dotted red area, the start and end of the dry seasons  
 373 are also indicated by a red vertical dotted line). Very wet periods occurs when the rainfall curve surpass  
 374 100 mm a month (in blue). The presence of savanna fires manually detected in the images is marked  
 375 with a flame symbol. The interruptions in the timeseries are due to technical problems with the  
 376 phenocams or with the weather station.

